On the Integration of Sub-6 Patch Antennas with Mm-Wave Reflectors

(Article begins on next page)

On the Integration of Sub-6 Patch Antennas with Mm-Wave Reflectors

Martin Petek
Dept. of Electronics and Telecommunications (DET)
Politecnico di Torino
Torino, Italy
martin.petek@polito.it

Francesca Vipiana
DET
Politecnico di Torino
Torino, Italy
francesca.vipiana@polito.it

Eva Rajo-Iglesias
Dept. of Signal Theory and Communication
University Carlos III of Madrid
Madrid, Spain
eva.rajo@uc3m.es

***Abstract*—In this work, we analyse the integration of a patch antenna operating at a lower frequency with a reflector antenna operating at a higher frequency, aiming to minimize the performance degradation of both. We first analyse the problem for the reflector antenna with geometric optics and derive an equation that defines the shape of the patch antenna surface. We then test the impact of such integration on both the side-lobe level and directivity with a full-wave solver. The results indicate an improvement in both compared to previous work.**

***Index Terms*—Geometrical optics, Multifrequency antennas, Reflector antennas**

I. Introduction

The global demand for high data rates, driven by video traffic in the telecommunication industry is increasing [1]. Therefore, to solve the problem of the congested sub-6 GHz bands, the fifth generation of mobile networks (5G) introduced use of the millimeter wave bands [2]. Traditionally, antennas for communication systems spanning two vastly different frequencies are typically designed and placed separately, which may lead to a prohibitively bulky structure.

This problem may be overcome with the co-design of both antennas such that the same aperture is utilized, in a way that mitigates the degradation of performance of both antennas to acceptable levels. Various methodologies have been proposed in previous works with this idea, for example, utilizing arrays [3], [4] or reflectarrays [5]. Reflector antenna designs are also proposed, such as in [6], where the same reflector is used for both frequencies, with the lower frequency source being located at the focal point and and the higher-frequency source is in a Cassegrain configuration. In [7], the idea of integrating a lower-frequency patch antenna with a higher-frequency reflector antenna is proposed. There, the patches are conformally placed on the surface of the reflector, at a distance of half the wavelength of the higher frequency.

In this work, we re-evaluate the proper approach to integrating a lower-frequency patch antenna with a higher-frequency reflector antenna. We start by analysing the problem with geometric optics to derive the optimal patch location and shape. Then, we study the effects of integration on both the reflector and patch antennas using full-wave numerical analysis. We demonstrate the improvement of our approach over [7] in terms of side-lobe level (SLL) and directivity, especially for the case where the patch antenna is placed at the edge of the reflector.

II. Geometrical Optics Analysis

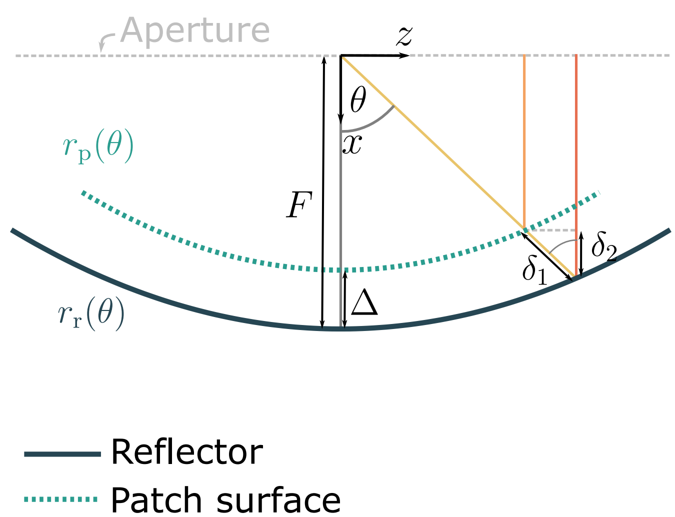

Fig. 1. Schematic of the problem analysed with geometric optics.

First, we analyse the problem of integration from the perspective of the higher frequency antenna, with wavelength λ_{H}. The geometry is presented in Fig. 1. In the figure, the yellow ray travels from the source, located at the focal point of the reflector, towards its surface r_{r}, defined with the parabolic equation

$$r_{\mathrm{r}} = \frac{F}{\cos^2(\theta/2)}. \tag{1}$$

Here, F is the focal distance. Without the patch surface, the ray reflects off the reflector and arrives in phase at the aperture for all θ. However, if the ray is instead reflected in the patch antenna, defined by the surface $r_{\mathrm{r}}(\theta)$, it travels a path shorter than $\delta_1 + \delta_2$, as marked in the figure. If this path is

$$\delta_1 + \delta_2 = n\lambda_{\mathrm{H}}, \tag{2}$$

where $n \in \mathbb{N}$ is a natural number, the ray will arrive in phase at the aperture. By noting that the angle between δ_1 and δ_2 is θ, we can express (2) as:

$$\delta_1 = \frac{n\lambda_\mathrm{H}}{1+\cos(\theta)} = \frac{n\lambda_\mathrm{H}}{2\cos^2(\theta/2)} \,. \tag{3}$$

The patch surface is therefore defined by:

$$r_\mathrm{p}(\theta) = r_\mathrm{r}(\theta) - \delta_1(\theta) = \frac{F - n\lambda_\mathrm{H}/2}{\cos^2(\theta/2)} \,, \tag{4}$$

which is a parabola with a focal distance $F - n\lambda_\mathrm{H}/2$. Note that, unlike in [7], this surface is not conformal to the high frequency reflector antenna.

III. Numerical Results

In this section, we evaluate the performance impact of the configuration proposed in the previous section. The operating frequency of the reflector and patch antennas is $f_\mathrm{H} = 28$ GHz and $f_\mathrm{L} = 3.5$ GHz, respectively. The geometry is presented in Fig. 2. The reflector antenna diameter is kept $D = 11.2\lambda_\mathrm{H}$ and the focal distance $F = 3.73\lambda_\mathrm{H}$. It is fed by a linearly polarized patch antenna. In the figure, w is the width of the low-frequency square patch on the zy plane and z_offset is the offset in z between the center of the patch and the center of the parabolic reflector. Two references are used to compare the performance of the reflector with the proposed patch surface in (4): only the reflector, or the patch following the approach from [7].

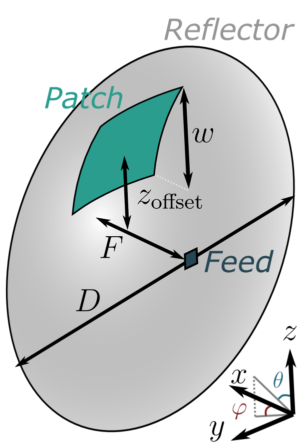

Fig. 2. Geometry of the antenna.

A. Impact on the reflector antenna performance

We now study the impact of the presence of the patch on the reflector antenna performance. First, we consider the case of the maximum offset of the patch $z_\mathrm{offset} = 30$ mm and $w = 38.5$ mm.

The vertical cut (fixed $\varphi = 0°$) of the directivity is depicted in Fig. 3. Without the patch, the reflector has a maximum directivity of 29.5 dB at $\theta = -90°$ and a SLL of -27.3 dB. Introducing the patch as in [7] reduces the directivity to 29 dB, slightly tilts the beam to $\theta = -89.8°$, and increases the SLL to -20.6 dB. Conversely, by using the surface proposed in (4), there is no beam tilt and both directivity and SLL degrade only slightly. Similar observations, with the exception of the beam tilt, can be made for the horizontal cut (fixed $\theta = 90°$) shown in Fig. 4.

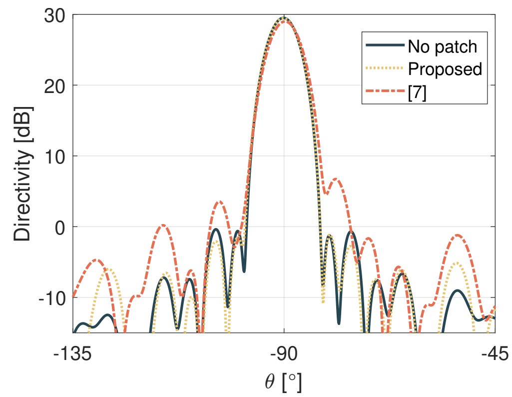

Fig. 3. Vertical cut (fixed $\varphi = 0°$) of the reflector antenna directivity.

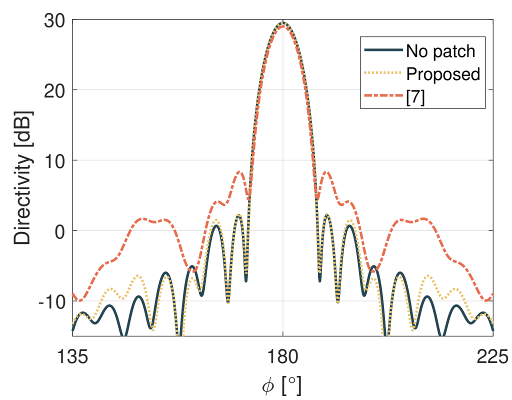

Fig. 4. Horizontal cut (fixed $\theta = 90°$) of the reflector antenna directivity.

We investigate this effect further by simulating the three surfaces separately. The results are presented in Fig. 5. There, we may note that the proposed patch surface reflects correctly in the same direction as the full reflector, while the conformal patch proposed in [7] redirects the beam 4° off the main lobe, resulting in both the beam tilt and an increased SLL as observed in Fig. 3.

The peak directivity and SLL as a function of the z_offset is presented in Fig. 6. First, we would like to note that, regardless of the patch location, the performance of the patch designed according to (4) is better for both the reflector and the patch itself, with improvements being more noticeable at the more extreme patch locations. Furthermore, we may note that the proposed inclusion of the patch does still degrade the reflector performance, especially when the patch is centrally located on the antenna. We attribute this to the effect of edge diffraction, which is not included in our geometrical optics analysis.

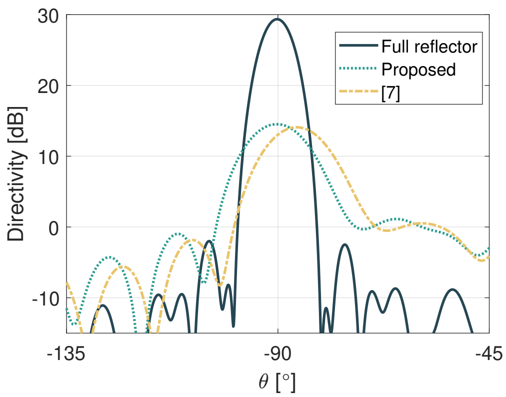

Fig. 5. Vertical cut (fixed $\varphi = 0°$) of the directivity for only the full reflector, the proposed patch, and the patch proposed in the previous work [7].

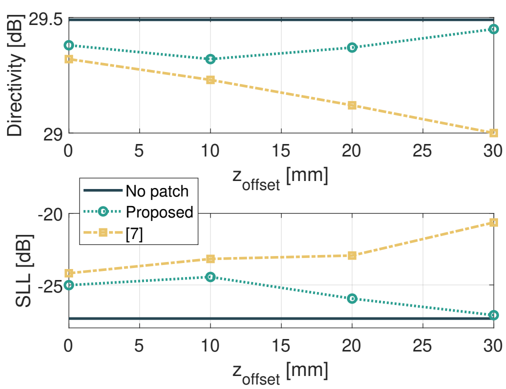

Fig. 6. Peak directivity (top) and SLL (bottom) of the reflector antenna for different locations of the patch.

B. Effect of integration on the patch

Since the patch is defined over a curved surface, w should be modified for each z_{offset} such that it radiates at $f_{\text{L}} = 3.5$ GHz. For the offsets $z_{\text{offset}} = \{0, 10, 20, 30\}$ mm, good matching is obtained with $w = \{0.43, 0.42, 0.41, 0.4\}\lambda_{\text{L}}$, where λ_{L} is the free-space wavelength at f_{L}. The computed reflection coefficient can be seen in Fig. 7. Good matching is achieved for all values of z_{offset}.

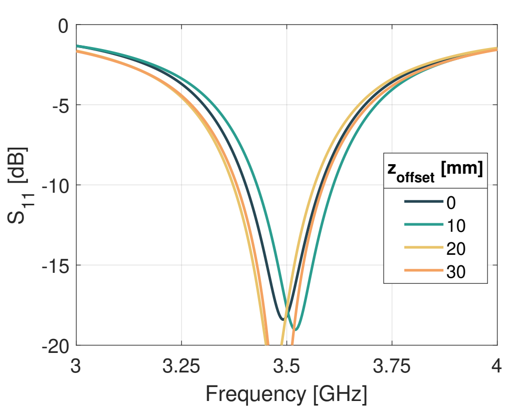

Fig. 7. Reflection coefficient of the patch antenna.

Another effect of the integration is beam tilt of the patch radiation as z_{offset} increases, as seen in the vertical cut of the farfield in Fig. 8. At the most extreme point, the beam tilt is $24°$. This can be exploited to implement a switched-beam system, but may also be undesired if radiation in the same direction as the reflector antenna is desired, as the directivity of the patch at broadside could be decreased by up to 3 dB.

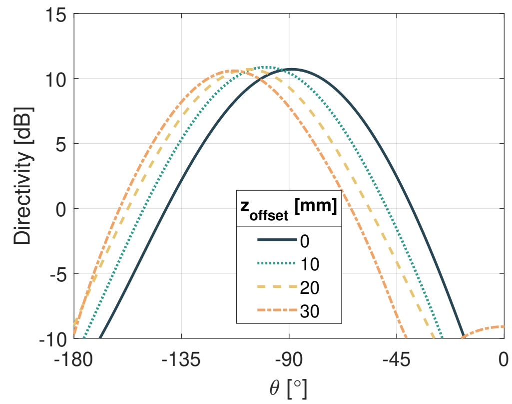

Fig. 8. Vertical cut (fixed $\phi = 0°$) of the patch antenna directivity.

C. Mutual coupling

Finally, we investigate any possible mutual coupling effects. The S_{12} for both lower and higher frequencies are depicted in Fig. 9. As seen in the figure, the mutual coupling is lower than -40 dB, implying the operation of one antenna should not significantly interfere with the other.

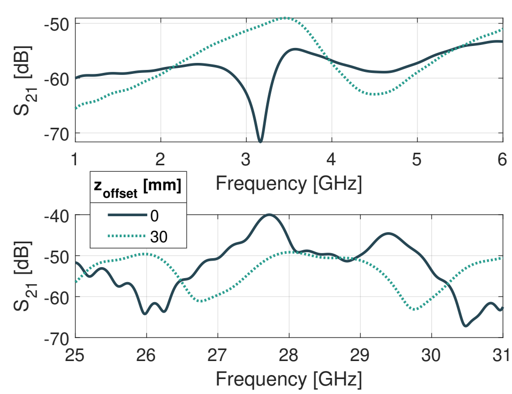

Fig. 9. Mutual coupling between the two antennas at the lower frequency (top) and higher frequency (bottom).

IV. Conclusion and Perspectives

In this work, we presented an alternative way to the solution presented in [7] to solve the problem of integration of a patch and a reflector antenna using geometric optics. Using a numerical full-wave solver, we demonstrated a new approach to improve the performance of the reflector antenna in terms of SLL and directivity.

In future work, we aim to design and manufacture a working prototype as well as address the issue of the tilting of the patch antenna's radiation pattern.

ACKNOWLEDGMENT

This publication is in part funded by the project "MedWaveImage - Microwave imaging technology transfer to innovate the medical sector", funded by Interreg Central Europe (CE0200670) and in part funded by the Spanish State Research Agency under project PID2022-141055NB-C22 from MCIN/AEI/10.13039/501100011033.

REFERENCES

[1] PwC, "Perspectives from the Global Telecom Outlook 2023–2027," PwC, Tech. Rep., 2023, accessed 06.07.2025. [Online]. Available: https://www.pwc.com/gx/en/industries/tmt/assets/pwc-gto-2023.pdf

[2] M. Agiwal, A. Roy, and N. Saxena, "Next Generation 5G Wireless Networks: A Comprehensive Survey," *IEEE Communications Surveys & Tutorials*, vol. 18, no. 3, pp. 1617–1655, 2016.

[3] F. Croq and D. Pozar, "Millimeter-wave design of wide-band aperture-coupled stacked microstrip antennas," *IEEE Transactions on Antennas and Propagation*, vol. 39, no. 12, pp. 1770–1776, 1991.

[4] E.-Y. Yim, D. Jang, C.-H. Lee, and H. Choo, "Design of an S/X-Band Single-Layer Shared-Aperture Array Antenna Using a Mutual Complementary Configuration," *Applied Sciences*, vol. 13, no. 7, 2023. [Online]. Available: https://www.mdpi.com/2076-3417/13/7/4379

[5] D. E. Serup, G. F. Pedersen, and S. Zhang, "Dual-Band Shared Aperture Reflectarray and Patch Antenna Array for S- and Ka-Bands," *IEEE Transactions on Antennas and Propagation*, vol. 70, no. 3, pp. 2340–2345, 2022.

[6] S. Chakrabarti and G. Barman, "An S-/Ka-Band Shared Aperture Tracking Reflector Antenna With Polarization Diversity," *IEEE Transactions on Antennas and Propagation*, vol. 69, no. 6, pp. 3165–3176, 2021.

[7] J.-M. Poyanco, A. Fernández-Durán, and E. Rajo-Iglesias, "Unified Design: Sub-6 GHz Conformal Patch Antennas Integrated With Millimeter-Wave Reflector for Fixed Wireless Access Terminals," *IEEE Transactions on Antennas and Propagation*, vol. 73, no. 1, pp. 635–640, 2025.